

PAPER

[View Article Online](#)
[View Journal](#) | [View Issue](#)Cite this: *RSC Adv.*, 2018, 8, 36445

Molecular keypad controlled circuit for Ce(III) and NO₃[−] ions recognition by μ w synthesized silicon-embedded organic luminescent sensor†

Navpreet Kaur,^a Gurjaspreet Singh,^b *^b Jasbhinder Singh,^a Akshpreet Singh,^b Pinky Satija,^b Gurpreet Kaur^c and Jandeep Singh *^a

This report demonstrates the mimicking of an electronic circuit diagram towards Ce(III) ion sensing response supported by molecular keypads. The probe naphthyl based triazole linked silatrane (NTS) was efficiently synthesized using a series of microwave mediated reactions. The luminescent sensor NTS was explored for the ion sensing response towards Ce(III) ions using DMSO and DMSO : H₂O 4 : 1 (v/v) as solvent media, respectively. The role of water in Ce(III) ion sensing was detected as 'turn-off' response that contradicts the 'turn-on' with DMSO. Further, the sensing of NO₃[−] ions by NTS–Ce(III) ensemble was associated with blue shift on absorption maxima. These mimicking response studies were sketched as circuit diagrams assisted by molecular keypad behaviour as IMPLICATION output logic gate.

Received 1st September 2018
Accepted 23rd October 2018

DOI: 10.1039/c8ra07294a

rsc.li/rsc-advances

Introduction

Ion recognition studies work upon the principle of fluctuation in absorption or emission maxima upon interactions of an ion(s) with an ionophore. The role of chemical sensing is the exploration of its applications in different disciplines of chemistry and are not limited to, clinical biology and environmental science. Among the numerous kinds of chemical sensors, luminescence-based chemosensors display a set of advantages, since they have high sensitivity (single ion detection), versatility (biocompatibility), low cost, easy application and good resolution, which are typical of photoluminescence spectroscopy.¹ A chemosensor has two basic units (a) the receptor unit for selective binding and (b) the signal unit for reporting output through change in the optical properties (Fig. 1). The detection of target analyte is achieved by the molecular recognition followed by signal transduction.² Among all type of compounds used as fluorescent chemosensors, organic luminophores are most widely studied due to their rich chemical structures, easy chemical modification and highly fluorescent quantum yield.^{3,4} The creation of luminophores through clean reaction methodologies have generated immense scientific interest in exploring copper(i)-catalyzed alkyne-azide cycloaddition (CuAAC).

There have been numerous citations pertaining to the transition metal ion sensing by using 1,2,3-triazoles but this is the first report (to the best of our knowledge) citing the use of 'Click Silylation' product for Ce(III) ion analysis.^{5–7} 'Click Silylation' technique introduced a terminal siloxy group into the luminophore bridged by 1,2,3-triazole linker.^{8–15} The naphthyl moiety (acting as active unit) linked *via* 1,2,3-triazole (spacer) has been explored as an ionic fluorophore can find potential application in bio-imaging technique owing to its specific excitation and emission UV values, unaltered by any interference from other metal ions.^{7,16,17} The triazole linker creates an effective link for host-guest binding yielding fluorescence quenching or enhancement, accompanied by batho- or hypso- chromic shift.⁵

Though cerium is classified as rare earth metal, it is still abundant in crust (66 $\mu\text{g g}^{-1}$) and has been put into use in metallurgy, vehicle catalytic converters, ceramic materials and as heterogenous catalyst. In contrary, Ce(III) ions hampers biological functioning by altering the immune systems and functioning of many essential body organs. The prolonged exposure to the moist areas rich in Ce(III) ions can cause lung embolisms and liver damage.^{18–21} Thus, there is an urgent need of selective sensor for analysis and recovery of Ce(III) ions in water, soil and industrial samples.²² The developments in cation sensing is interlinked to anion sensing and are driven by their major role in biology, industry and environment pollution. Anion sensing works on the displacement module where an anion binds to receptor by replacing an indicator, causing perturbations in absorption spectral values.^{23–25} The Schiff base framework acts as the backbone to assists binding of anions that may result into the significant visual changes after complexation.^{26–29}

The mimicking of sensing behaviour can be processed as '0' and '1' input values in case of logic gates that is instantly

^aDepartment of Chemistry, Lovely Professional University, Phagwara-144411, Punjab, India. E-mail: singhjandeep@gmail.com; Tel: +91 9815967272

^bDepartment of Chemistry and Centre of Advanced Studies in Chemistry, Panjab University, Chandigarh-160014, India

^cDepartment of Chemistry, Gujranwala Guru Nanak Khalsa College, Civil Lines, Ludhiana-141001, India

† Electronic supplementary information (ESI) available. See DOI: 10.1039/c8ra07294a

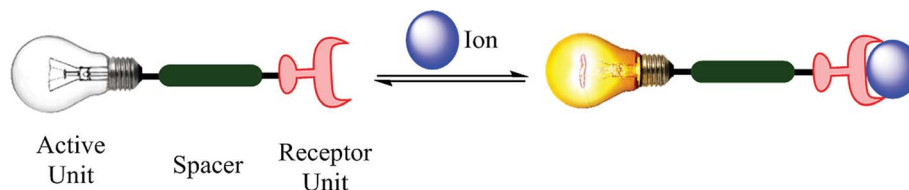


Fig. 1 Representation of a fluorescent ion luminescent sensor.

processed by specific output changes as signals of molecular gates.^{15,30–33} So, far no Ce(III) ion-ensemble sensing nitrate ions have been reported to the best of our knowledge. Thus, we herein report a new silicon capped 1,2,3-triazole linked naphthyl luminescent sensor (NTS) with regulated ON–OFF–ON switch module towards Ce(III) and NO_3^- ions. This type of behaviour has been mapped with the working of molecular switches that can work with an appropriate combination of chemical inputs.

Experiment

Materials and methods

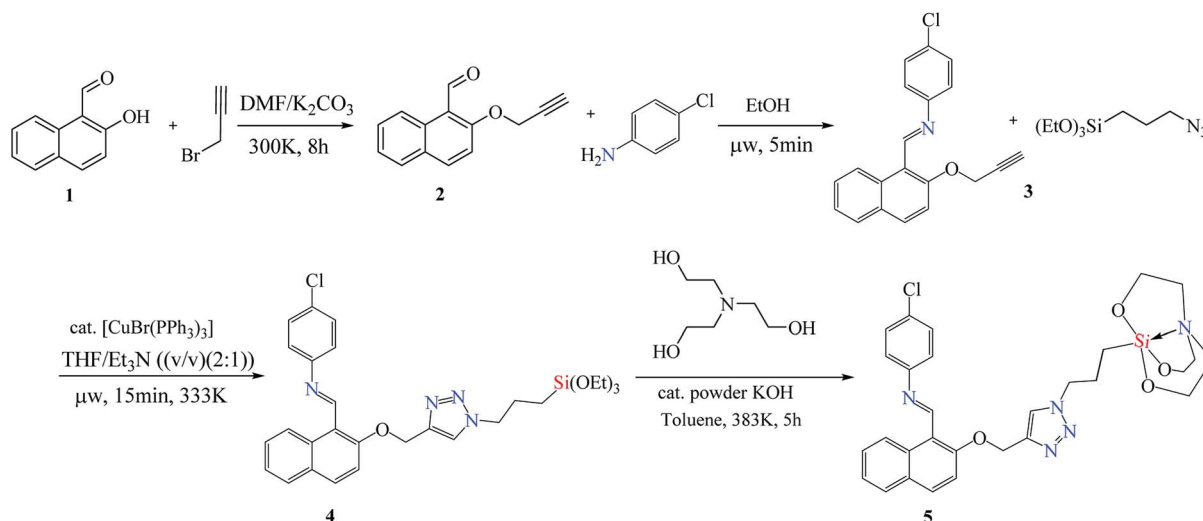
All the syntheses were carried out under inert dry nitrogen atmosphere using vacuum glass line. The organic solvents were dried according to standard procedures.³⁴ 2-Hydroxy-1-naphthaldehyde (Aldrich), 4-chlorobenzenamine (Aldrich), bromotris (triphenylphosphine) copper(I) $[\text{CuBr}(\text{PPh}_3)_3]$ (Aldrich), tetrahydrofuran (THF) (CDH), triethylamine (Et_3N) (SDFCL), triethanolamine (CDH), KOH (CDH), toluene (SDFCL), DMF (FINAR) were used as received. 3-Azidopropyltriethoxysilane (AzPTES) was synthesized by known procedure from literature.^{35,36} Infrared spectrum was obtained neat on a Thermo Scientific Fischer spectrometer. CHN analysis was obtained on Perkin Elmer Model 2400 CHNS elemental analyzer and Thermo Scientific Flash 2000 organic elemental analyzer. Multinuclear NMR (^1H , ^{13}C) spectra were recorded on a Bruker advance II 400 and on a Jeol (AL 300 MHz) spectrometer using CDCl_3 as internal reference and chemical shifts were reported

relative to tetramethylsilane. Melting points were uncorrected and measured in a Mel Temp II device using sealed capillaries.

Synthesis of luminescent sensor 5

The entity 2 (Scheme 1) was synthesised from 2-hydroxy-1-naphthaldehyde 1 by a known procedure.^{36–39} The entity 3 was synthesized by microwave upon reacting equimolar quantity of 4-chloroaniline (0.18 g, 1.4 mmol) with 2 (0.3 g, 1.4 mmol) using 1 ml of ethanol as solvent at 60 °C. The yellow coloured solid product 3 was obtained within five minutes. The Schiff base alkyne 3 (0.38 g, 1.2 mmol) was treated with 3-azidopropyltriethoxysilane (0.29 g, 1.2 mmol) in equimolar ratio using THF : TEA 2 : 1 (v/v) (optimized as entry 2 in Table 1) as solvent and $[\text{CuBr}(\text{PPh}_3)_3]$ as catalyst (0.01 mmol/alkyne function) in microwave at 60 °C for 15 minutes. The 1,4 triazole linked naphthyl terminated triethoxysilane 4 was extracted by solvent evaporation after catalyst filtration as stereospecific product.⁴⁰ The silane 4 (0.63 g, 1.1 mmol) was processed by transesterification reaction with triethanolamine (0.18 g, 1.2 mmol) using toluene as solvent and anhydrous powdered KOH as catalyst to yield silatrane 5.

Synthesis of 3. Yield: 84%; mp: 121–122 °C; anal. calcd for $\text{C}_{20}\text{H}_{14}\text{ClNO}$ (%): C, 75.12; H, 4.41; N, 4.38; found (%): C, 74.68; H, 4.51; N, 4.02. IR (neat, cm^{-1}): 2920, 2943, 2986, 2828, 2041, 1474, 1397, 1113, 947, 787; ^1H NMR (300 MHz, CDCl_3) δ = 9.48 (d, J = 8.7 Hz, 1H), 9.15 (s, 1H), 7.87 (d, J = 9.1 Hz, 1H), 7.71 (d, J = 8.0 Hz, 1H), 7.51 (t, J = 7.3 Hz, 1H), 7.36 (d, J = 7.5 Hz, 1H), 7.31 (d, J = 4.8 Hz, 2H), 7.16 (t, J = 6.4 Hz, 2H), 4.83 (d, J = 2.3 Hz, 2H), 3.64 (s, 1H), 2.42 (t, J = 4.1 Hz, 1H).



Scheme 1 Reaction sequence followed for the synthesis of luminescent sensor NTS (5).



Table 1 Optimization of reaction conditions for μ w assisted synthesis of triazole

Entry	Solvent ratio	Reaction duration (μ w)	Yield ^a (%)
1	THF : TEA 1 : 1 (v/v)	15 min	81
2	THF : TEA 2 : 1 (v/v)	15 min	93
3	THF : TEA 1 : 2 (v/v)	15 min	67
4	THF : TEA 3 : 1 (v/v)	15 min	74
5	THF : TEA 1 : 1 (v/v)	30 min	82
6	THF : TEA 2 : 1 (v/v)	30 min	93
7	THF : TEA 1 : 2 (v/v)	30 min	72
8	THF : TEA 3 : 1 (v/v)	30 min	79

^a Determined by ^1H NMR analysis of isolation of crude sample.

Synthesis of 4. Yield 93%; viscous brown oil; anal. calcd for $\text{C}_{29}\text{H}_{35}\text{ClN}_4\text{O}_4\text{Si}$ (%): C, 61.41; H, 6.22; N, 9.88; found (%): C, 61.38; H, 6.41; N, 9.25; IR (neat, cm^{-1}): 2931, 2867, 2831, 1645, 1606, 1576, 1361, 1301, 1165, 1077, 1023, 887, 831, 797, 691; ^1H NMR (300 MHz, CDCl_3) δ = 9.45 (d, J = 8.7 Hz, 1H), 9.10 (s, 1H), 7.80 (d, J = 9.0 Hz, 1H), 7.64 (d, J = 8.0 Hz, 1H), 7.49–7.40 (m, 2H), 7.36–7.22 (m, 4H), 7.09 (d, J = 8.6 Hz, 2H), 5.32 (s, 2H), 4.21 (t, J = 7.1 Hz, 2H), 3.66 (q, J = 7.0 Hz, 6H), 1.95–1.81 (m, 2H), 1.09 (t, J = 7.0 Hz, 9H), 0.50–0.33 (m, 2H); ^{13}C NMR (101 MHz, CDCl_3) δ = 158.79, 158.43, 151.66, 134.04, 132.26, 131.94, 131.81, 131.02, 129.42, 129.14, 128.53, 128.47, 128.33, 125.91, 124.60, 122.35, 117.59, 114.20, 67.91, 63.52, 58.50, 57.98, 52.47, 25.59, 24.17, 18.42, 18.29, 7.40.

Synthesis of 5. Yield 87%; mp: 231–233 °C (decom.); anal. calcd for $\text{C}_{29}\text{H}_{32}\text{ClN}_5\text{O}_4\text{Si}$ (%): C, 60.25; H, 5.58; N, 12.1; found (%): C, 59.78; H, 5.82; N, 12.27; IR (neat, cm^{-1}): 2858, 1683, 1370, 1323, 1058, 977, 764, 577; ^1H NMR (300 MHz, CDCl_3) δ =

9.46 (d, J = 8.9 Hz, 1H), 9.16 (s, 1H), 7.86 (d, J = 9.0 Hz, 1H), 7.70 (d, J = 7.9 Hz, 2H), 7.60 (s, 1H), 7.52–7.39 (m, 4H), 7.13 (d, J = 8.4 Hz, 2H), 5.34 (s, 2H), 4.22 (t, J = 7.2 Hz, 2H), 3.60 (t, J = 5.7 Hz, 6H), 2.69 (t, J = 5.7 Hz, 6H), 1.99–1.71 (m, 2H), 0.33–0.17 (m, 2H); ^{13}C NMR (101 MHz, CDCl_3) δ = 158.94, 158.59, 151.77, 142.93, 134.08, 131.85, 130.98, 129.34, 129.13, 128.61, 128.54, 128.35, 125.89, 124.55, 122.93, 122.46, 122.37, 117.58, 114.27, 63.75, 57.49, 56.79, 53.46, 50.94, 26.31, 13.20; MS (ES^+) calcd for $[\text{M} + \text{H}]^+$ 578.19; found 578.18.

Results and discussion

Synthesis

The base catalysed nucleophilic substitution of 2-hydroxy-1-naphthaldehyde (**1**) with propargyl bromide resulted into an alkyne terminated product **2**. This alkyne product was separated and was subjected to the microwave promoted condensation reaction with 4-chloroaniline yielding a Schiff base product **3** with terminal alkyne fragment. The Schiff base alkyne **3** with irradiated with microwaves in the presence of Cu(I) that catalysed cycloaddition reaction with 3-azidopropylsilane. The THF : TEA 2 : 1 (v/v) acted as solvent media and the reaction was complete within 15 minutes at the temperature of 60 °C. The resulting cyclo-addition product obtained contains 1,2,3-triazole linker with terminal ethoxysilyl group **4** in good yield. This product is hydrolytically unstable which restricts its reactivity and application in water-based systems. Thus, ethoxysilyl group was replaced by an atrane ring **5** by trans-esterification reaction, making it stable for use in various aqueous mediums. This luminescent sensor **5** was further used for chemo-sensing studies (labelled as NTS).

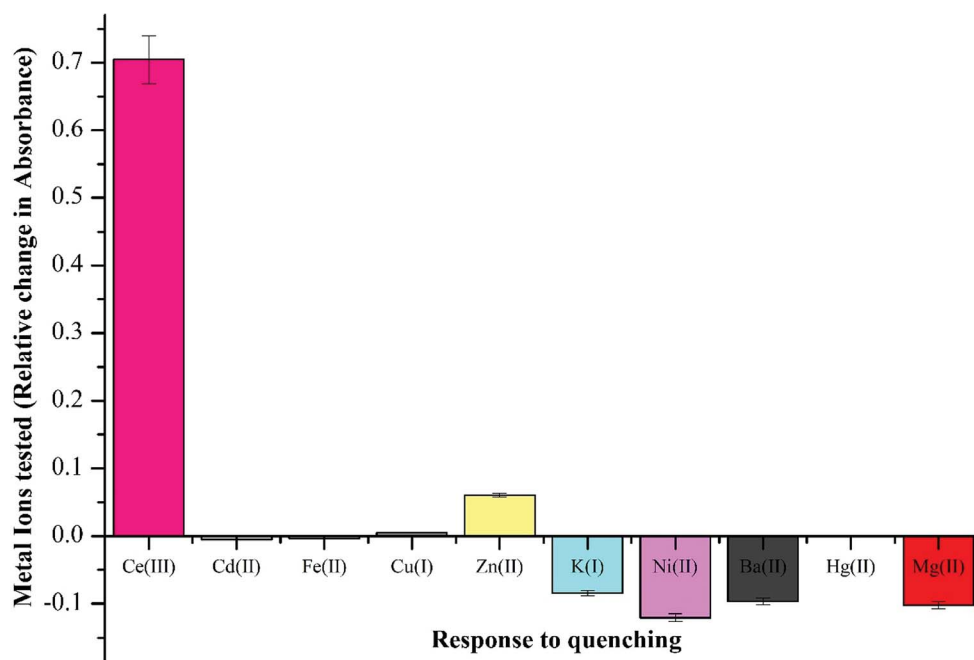


Fig. 2 Competitive absorbance response recorded by luminescent sensor NTS with different cationic species using DMSO : H_2O 4 : 1 (v/v) by addition of 5 equiv. of 20 μM metal ion solution with recorded change in maxima value at $\lambda = 322$ nm.



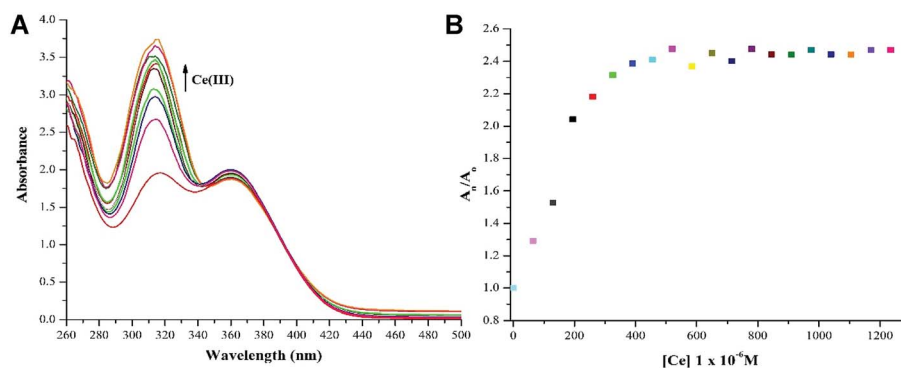


Fig. 3 (a) 'Turn-on' response ($\lambda_{\text{max}} = 322 \text{ nm}$) recorded with successive addition of $60 \mu\text{M}$ solution of Ce(III) ions using DMSO as solvent owing to NTS– Ce(III) ion interactions; (b) relative change in absorption maxima (A_n/A_o) with addition of 15 equiv. of $20 \mu\text{M}$ of Ce(III) ions; (A_o = absorption maxima of NTS; A_n = absorption maxima with successive addition of Ce(III) ions).

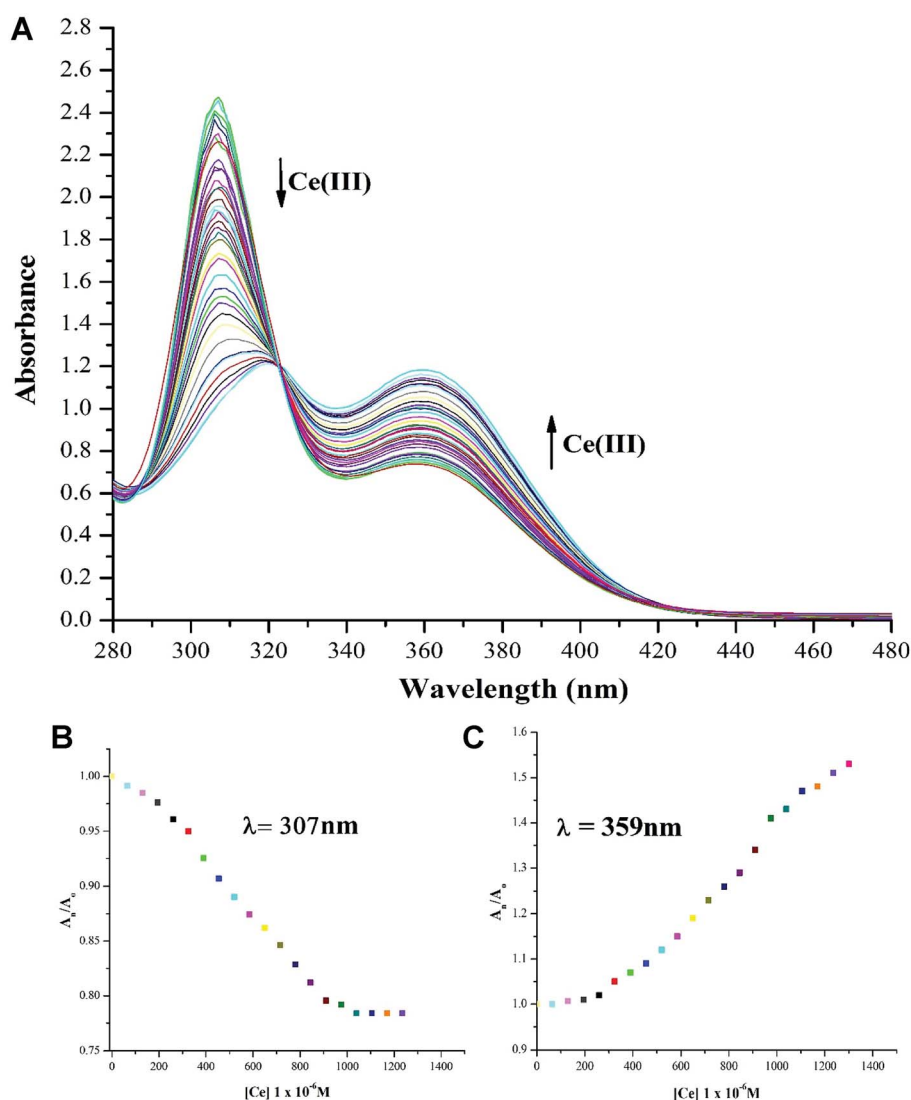


Fig. 4 (a) 'Turn-off' response ($\lambda_{\text{max}} = 307 \text{ nm}$) associated with red shift (to $\lambda_{\text{max}} = 319 \text{ nm}$) recorded with successive addition of $20 \mu\text{M}$ solution of Ce(III) ions using DMSO : H_2O 4 : 1 (v/v) as solvent owing to NTS– Ce(III) ion interaction which is associated with "turn-on" response ($\lambda_{\text{max}} = 359 \text{ nm}$) creating an isosbestic point at 322 nm ; (b) relative change in absorption maxima (A_n/A_o) with ($\lambda_{\text{max}} = 307 \text{ nm}$) upon addition of 30 equiv. of $20 \mu\text{M}$ of Ce(III) ions; (c) relative change in absorption maxima (A_n/A_o) with ($\lambda_{\text{max}} = 359 \text{ nm}$) upon addition of 30 equiv. $20 \mu\text{M}$ of Ce(III) ions; (A_o = absorption maxima of NTS; A_n = absorption maxima with successive addition of Ce(III) ions).



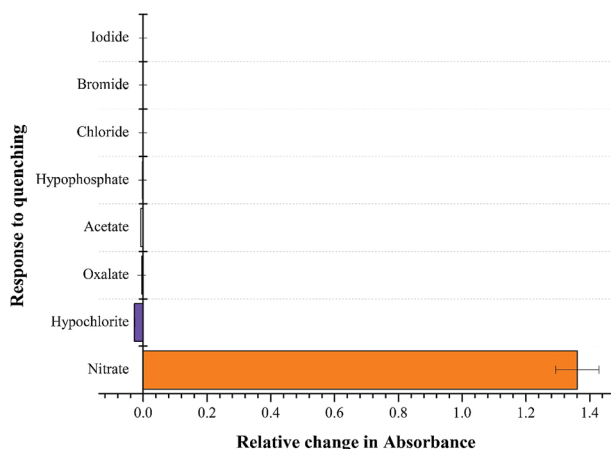


Fig. 5 Competitive absorbance response recorded by excimer NTS–Ce(III) complex with different anionic species using DMSO : H₂O 4 : 1 (v/v) by addition of 5 equiv. of 13 μ M anionic solutions with recorded change in maxima value at $\lambda = 319$ nm.

UV-vis spectra

Cationic sensing. The absorbance spectral properties of NTS were examined solvatochromically using chloroform, dimethyl sulfoxide, dimethylformamide, and methanol, which demonstrated dimethyl sulfoxide to be the most suited solvent for photochromic analysis, owing to solubility and better detection studies. To record the metal-ion effect on absorption spectrum of NTS, 20 μ M concentration of Ce(III), Cd(II), Fe(II), Cu(I), Zn(II), K(I), Ni(II), Ba(II), Hg(II), Mg(II) and Ag(I) ions were prepared and analysed in DMSO : H₂O 4 : 1 (v/v). This demonstrated negligible quenching in absorption wavelength maxima, except for Ce(III) ions, where a large stimulated change was recorded as plotted in Fig. 2. The activity of Ce(III) ions in comparison to other metal ions owes to $6s^2 4f^1 5d^1$ electronic configuration wherein the high energy of $4f-5d$ configuration (6.3 eV) makes it more reactive. The quenching response of Ce(III) ions is proposed to proceed through electron or energy transfer due to presence of unpaired electrons.^{41,42}

The ion sensing study was analysed in two different solvent media *i.e.* DMSO and DMSO : H₂O 4 : 1 (v/v). The successive

addition of 15 equivalent of 20 μ M Ce(III) in DMSO yielded a hyperchromic shift in the absorption maxima, commonly referred to as “turn-on” output optical response. The comparative “turn-on” behaviour among each peak decreased upon successive addition of Ce(III) ions, which can be attributed to Internal Charge Transfer (ICT) interaction of NTS with Ce(III) ions. The relative changes in absorption maxima with increasing Ce(III) ion concentration have been shown in Fig. 3.

To explore the utility of NTS in water based systems, the absorption maxima values were recorded and plotted for NTS with solvent mixture of DMSO : H₂O 4 : 1 (v/v) as shown in Fig. 4. The studies performed with DMSO : H₂O 4 : 1 (v/v) exhibit “turn-off” for absorption maxima at 319 nm accompanied by a blue shift to 307 nm. This titration process creates an isosbestic point at 322 nm accompanied by “turn-on” response for absorption maxima with λ_{max} of 359 nm, indicating the production of single component in response to NTS and Ce(III) ion interactions. This observation can be attributed to the role of water interfering with NTS–Ce(III)–DMSO interactions in the solvent mixture. The lowest detection limit of analysis of Ce(III) ions using NTS probe is 60 μ M.

Anionic sensing. NTS–Ce(III) ensemble was tested for anion sensitivity using 13 μ M solutions of different anions: NO_3^- , OCl^- , $\text{C}_2\text{O}_4^{2-}$, CH_3COO^- , Cl^- , Br^- , I^- in DMSO : H₂O 4 : 1 (v/v) as shown in Fig. 5. The change in absorbance was observed with equimolar additions of NO_3^- ions whereas insignificant changes were observed with OCl^- ions and no change was recorded with rest of the anions. The high selectivity displayed by rise in absorption maxima corresponds to “turn-on” response module for NTS–Ce(III)– NO_3^- system. There was recovery of original absorption maxima upon addition of 5 equiv. (13 μ M) solution of NO_3^- ions solution (Fig. 6). This chemo-sensing of anions using metals have been credited to photo electron transfer (PET) from receptor to luminescent sensor. The metal ion pre-organizes the complex to have a geometry compatible with host–guest binding. The lanthanide ensembles provide a platform for effective anion sensing in water, since aqua molecules being present in vacant coordination site can be displaced by anions. Thus, leading to spectral variations in metal-ensemble-anion system.^{23–25} On

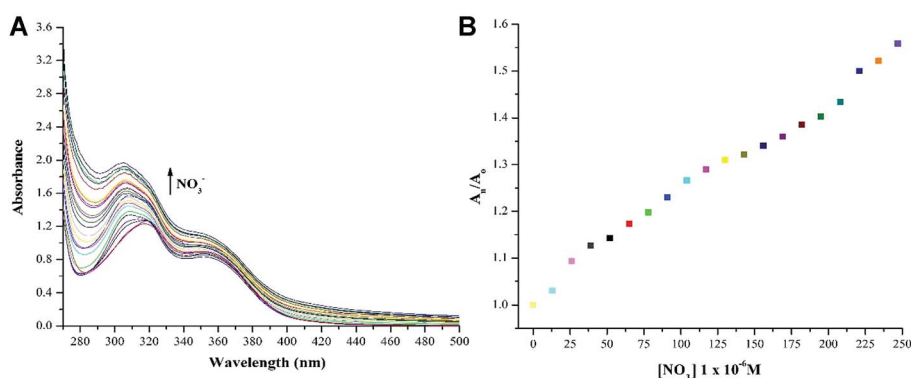


Fig. 6 (a) “Turn-on” response ($\lambda_{\text{max}} = 322$ nm) associated with blue shift (to $\lambda_{\text{max}} = 305$ nm) was recorded with the successive addition of 10 μ M solution of NO_3^- ions using DMSO : H₂O 4 : 1 (v/v) as solvent which is a result of [NTS–Ce(III)] – NO_3^- ion interactions; (b) relative change in absorption maxima (A_n/A_0) with addition of 13 μ M of NO_3^- ions; (A_0 = absorption maxima of NTS–Ce(III) ions; A_n = absorption maxima with successive addition of NO_3^- ions).



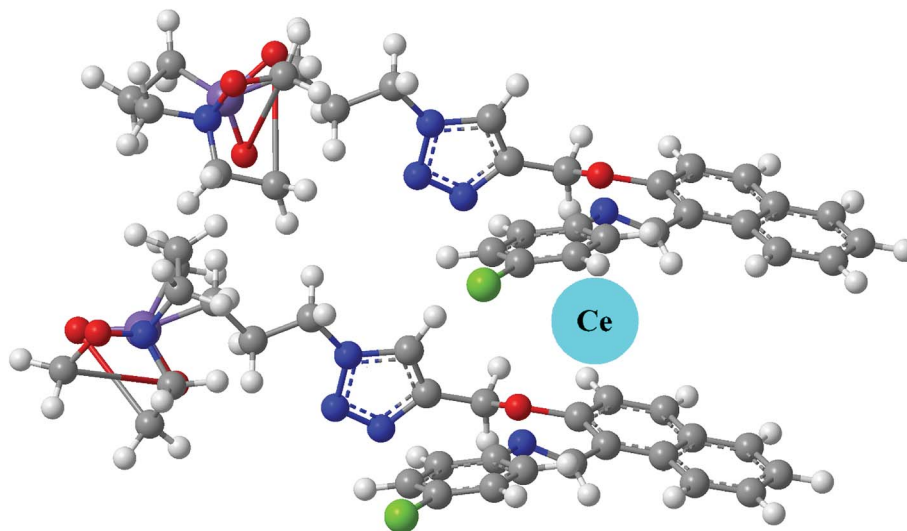


Fig. 7 The binding mode of Ce^{3+} ions with NTS luminescent sensor.

Ce^{3+}	NO_3^-	Output	Logic gate
0	0	1	
0	1	0	
1	0	1	
1	1	1	

Fig. 8 The relative absorbance intensity change observed with NTS upon addition of Ce^{3+} and NO_3^- ions with '0' and '1' signifying 'no change in λ_{max} ' and 'turn-off/turn-on' response, respectively; along with the mimicking of response as IMPLICATION logic gate.

this basis, an expected binding mode was sketched (Fig. 7) with NTS : $\text{Ce}(\text{III})$ ion binding in 1 : 1 fashion.

Expected binding mode

NTS have been used as cationic chemo-sensor for cerium ion recognition, followed by nitrate ion assimilation. In order to render insight into the structural features, the geometry of ligand was optimised at DFT/B3LYP/6-31G level of theory. The optimized geometry had all frequencies indicating that obtained structure is a global minimum. Since, the binding of cerium as $\text{Ce}(\text{III})$ depends upon the size of supramolecular cavity, it must held together by two molecules in a layered structure as shown in Fig. 7. This is supported by a fact that $\text{Ce}(\text{III})$ is a larger ion, it cannot fit into a smaller cavity created by a single NTS molecule.⁷ Thus, the expected binding stoichiometric ratio for NTS : $\text{Ce}(\text{III})$ is 2 : 1.

Molecular keypad mimicking

The plotting of ionic response as Boolean function by performing logical operation produces a response that can be

implemented as an electronic switch control. These binding studies inspire us to design a [(receptor)–(Ce^{3+})–(NO_3^-)] binding model using molecular keypad. The simplification of input signal and output response as molecular keypad was designed as shown in Fig. 8. An alternate way of sensing behaviour for NTS was performed using NTS– NO_3^- followed by successive addition of 20 μM of $\text{Ce}(\text{III})$. The rise in signal intensity was observed with a pattern similar to that observed for NTS– $\text{Ce}(\text{III})$ ensemble. These results evidently highlight the two-way sensing of both NO_3^- ions.

Circuit diagram

The developments in electrical circuits to simplify the ion sensing behaviour will attract considerable scientific interest. The response obtained can be drafted as circuit board diagram (as shown in Fig. 9) with NTS as sensing unit and $\text{Ce}(\text{III})$ and NO_3^- ions as keys for circuit completion. The addition of $\text{Ce}(\text{III})$ to NTS results into a change in absorption maxima whereas NO_3^- ions do not alter the λ_{max} value. Further, the addition of NO_3^- ions into NTS– $\text{Ce}(\text{III})$ ensemble or Ce^{3+} ions to NTS– NO_3^- ensemble depicts significant change in absorption maxima.



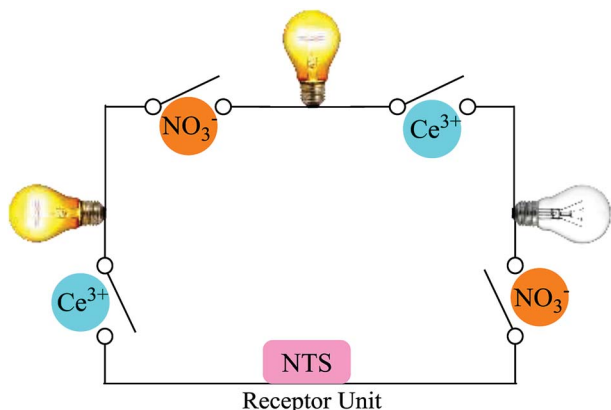


Fig. 9 Ions controlled circuit diagram as a response with NTS.

Conclusion

The use of microwave radiations to create NTS luminescent sensor paved an effective pathway for clean, quick and efficient synthesis. The chemo-sensing of Ce(III) ions in DMSO and $\text{DMSO} : \text{H}_2\text{O} 4 : 1$ (v/v) solvent system resulted into the unique 'turn-on' and 'turn-off' responses, respectively. This ensemble was further utilised for NO_3^- ion detection with a 'turn-off' response. The N, O, N cornered caged is generated that can efficiently trap Ce(III) ions till the lower concentration limit of $60 \mu\text{M}$. This behaviour of NTS- Ce(III) - NO_3^- system is mimicked as IMPLICATION logic gate that can be simplified as a circuit diagram.

Conflicts of interest

There are no conflicts to declare.

Acknowledgements

We are thankful to Mrs Renki and Mr Manoj for helping us with UV-vis data collection.

References

- 1 L. Prodi, F. Bolletta, M. Montalti and N. Zaccheroni, *Coord. Chem. Rev.*, 2000, **205**(1), 59.
- 2 C. Bargossi, M. C. Fiorini, M. Montalti, L. Prodi and N. Zaccheroni, *Coord. Chem. Rev.*, 2000, **208**(1), 17.
- 3 G. Kaur, G. Singh and J. Singh, *Mater. Today Chem.*, 2018, **8**, 56.
- 4 Q. Zhao, F. Li and C. Huan, *Chem. Soc. Rev.*, 2010, **39**(8), 3007.
- 5 Y. H. Lau, P. J. Rutledge, M. Watkinson and M. H. Todd, *Chem. Soc. Rev.*, 2011, **40**(5), 2848.
- 6 L. B. Desmonts, D. N. Reinhoudt and M. C. Calama, *Chem. Soc. Rev.*, 2007, **36**(6), 993.
- 7 M. Panchal, A. Kongor, M. Athar, V. Mehta, P. C. Jha and V. K. Jain, *New J. Chem.*, 2018, **42**(1), 311.
- 8 G. Singh, S. S. Mangat, J. Singh, A. Arora and M. Garg, *J. Organomet. Chem.*, 2014, **769**, 124.
- 9 G. Singh, S. S. Mangat, J. Singh, A. Arora and R. K. Sharma, *Tetrahedron Lett.*, 2014, **55**(4), 903.
- 10 G. Singh, S. S. Mangat, H. Sharma, J. Singh, A. Arora, A. P. S. Pannu and N. Singh, *RSC Adv.*, 2014, **4**(69), 36834.
- 11 G. Singh, A. Arora, S. S. Mangat, J. Singh, S. Chaudhary, N. Kaur and D. C. Lazarte, *J. Mol. Struct.*, 2014, **1079**, 173.
- 12 G. Singh, J. Singh, S. S. Mangat and A. Arora, *Tetrahedron Lett.*, 2014, **55**(15), 2551.
- 13 G. Singh, J. Singh, S. S. Mangat, J. Singh and S. Rani, *RSC Adv.*, 2015, **5**(17), 12644.
- 14 G. Singh, J. Singh, S. S. Mangat and A. Arora, *RSC Adv.*, 2014, **4**, 60853.
- 15 G. Singh, J. Singh, J. Singh and S. S. Mangat, *J. Lumin.*, 2015, **165**, 123.
- 16 J. Hatai, M. Samanta, V. S. R. Krishna, S. Pal and S. Bandyopadhyay, *RSC Adv.*, 2013, **3**(44), 22572.
- 17 M. Liu, Z. Xu, Y. Song, H. Li and C. Xian, *J. Lumin.*, 2018, **198**(1), 337.
- 18 H. X. Mai, Y. W. Zhang, R. Si, Z. G. Yan, L. D. Sun, L. P. You and C. H. Yan, *J. Am. Chem. Soc.*, 2006, **128**(19), 6426.
- 19 A. Afkhami, T. Madrakian, A. Shirzadmehr, M. Tabatabaee and H. Bagheri, *Sens. Actuators, B*, 2012, **174**, 237.
- 20 M. R. Awual, M. M. Hasan, A. Shahat, M. Naushad, H. Shiwaku and T. Yaita, *Chem. Eng. J.*, 2015, **265**, 210.
- 21 G. Tyler, *Plant Soil*, 2004, **267**(1), 191.
- 22 M. Shamsipur, M. Yousefi and M. R. Ganjali, *Anal. Chem.*, 2000, **72**(11), 2391.
- 23 P. A. Gale and C. Caltagirone, *Chem. Soc. Rev.*, 2015, **44**(13), 4212.
- 24 S. Shinoda and H. Tsukube, *Analyst*, 2011, **136**(3), 431.
- 25 V. Borse, P. Jain, M. Sadawana and R. Srivastava, *Sens. Actuators, B*, 2016, **225**, 340.
- 26 N. Mishra, K. Poonia, S. K. Soni and D. Kumar, *Polyhedron*, 2016, **120**, 60.
- 27 Y. M. Hijji, B. Barare, A. P. Kennedy and R. Butcher, *Sens. Actuators, B*, 2009, **136**(2), 297.
- 28 C. G. Neochoritis, T. Z. Tzitzikas, C. A. Tsoleridis, J. S. Stephanatou, C. A. Kontogiorgis, D. J. H. Litina and T. C. Papadopoulou, *Eur. J. Med. Chem.*, 2011, **46**(1), 297.
- 29 O. A. Bozdemir, R. Guliyev, O. Buyukcikir, S. Selcuk, S. Kolemen, G. Gulseren and E. U. Akkaya, *J. Am. Chem. Soc.*, 2010, **132**(23), 8029.
- 30 Y. Wang, Y. Huang, B. Li, L. Zhang, H. Song, H. Jiang and J. Gao, *RSC Adv.*, 2011, **1**(7), 1294.
- 31 V. Bhalla and M. Kumar, *Org. Lett.*, 2012, **14**(11), 2802.
- 32 Q. Li, Y. Yue, Y. Guo and S. Shao, *Sens. Actuators, B*, 2012, **173**, 797.
- 33 B. Chen, L. Wang, F. Zapata, G. Qian and E. B. Lobkovsky, *J. Am. Chem. Soc.*, 2008, **130**, 6718.
- 34 A. I. A. Vogel, *A Text Book of Practical Organic Chemistry*, Longman, London, 4th edn, 1978.
- 35 A. Bianco, M. Maggini, M. Nogarole and G. Scorrano, *Eur. J. Org. Chem.*, 2006, **13**, 2934.
- 36 L. X. Cheng, J. J. Tang, H. Luo, X. L. Jin, F. Dai, J. Yang and B. Zhou, *Bioorg. Med. Chem. Lett.*, 2010, **20**(8), 2417.



- 37 G. A. Harrison, S. Zhou, J. V. Hines and S. C. Bergmeier, *J. Comb. Chem.*, 2010, **12**(4), 491.
- 38 M. J. Khoshkholgh, S. Balalaie, R. Gleiter and F. Rominger, *Tetrahedron*, 2008, **64**(48), 10924.
- 39 G. Singh, P. Kalra, A. Arora, Sanchita, G. Sharma, A. Singh and V. Verma, *Inorg. Chim. Acta*, 2018, **473**, 186.
- 40 H. C. Kolb, M. G. Finn and K. B. Sharpless, *Angew. Chem., Int. Ed.*, 2001, **40**, 2004.
- 41 E. Priyadarshini, N. Pradhan, P. Panda and B. Mishra, *Biosens. Bioelectron.*, 2015, **68**, 598.
- 42 C. Duran, A. Gundogdu, V. N. Bulut, M. Soylak, L. Elci, H. B. Sentürk and M. Tüfekci, *J. Hazard. Mater.*, 2007, **146**, 347.

